Clin Oral Invest (2015) 19:1595–1603
DOI 10.1007/s00784-014-1385-0

ORIGINAL ARTICLE

Tissue reactions after simultaneous alveolar ridge augmentation with biphasic calcium phosphate and implant insertion—histological and immunohistochemical evaluation in humans

Anton Friedmann · Kirsten Gissel · Anna Konermann · Werner Götz

Received: 11 June 2014 / Accepted: 3 December 2014 / Published online: 17 December 2014

Abstract
Objectives Simultaneous lateral augmentation and implant placement is considered as standard procedure in deficient edentulous ridges in oral implantology. Histological studies monitoring osteogenesis after application of alloplastic bone substitutes in humans are scarce. Bone formation upon simultaneous augmentation with biphasic calcium phosphate (BCP) and implantation was histologically investigated after 6 months in situ. The results of this secondary analysis are reported tempting to ascribe specific observations to uneventful submerged healing or compromised healing of soft tissues including occurrence of dehiscences and premature graft exposure.
Materials and methods Histology of biopsies from lateral, crestal bone augmentations using alloplastic BCP comprising seven sites with compromised, prematurely exposed healing and six sites with uneventful submerged healing was investigated for expression of osteogenic, osteoclastogenic, and angiogenic differentiation markers.
Results Histology revealed alkaline phosphatase (ALP)-positive osteoblasts and immunoreactivity for osteogenic markers osteocalcin and collagen type I in biopsies with submerged healing, while inflammatory infiltrates and accumulations of multinucleated giant cells around BCP granules were observed in compromised sites. All specimens presented adequate vessel density. Multinucleated giant cells showed inconsistent staining for the osteoclast marker tartrate-resistant acid phosphatase (TRAP).
Conclusions The histological findings of this study indicate an osteoconductive nature of the BCP applied. Premature exposure of the bone substitute reduced new bone formation and may bear a risk for inflammatory and foreign body reactions.
Clinical relevance A predictable appositional bone formation in simultaneously augmented sites using BCP is linked to an uneventful healing process.

Keywords Dental implants · Guided bone regeneration · Simultaneous alveolar ridge augmentation · Healing

Introduction

Simultaneous augmentation is an approach of guided bone regeneration (GBR) implying implant placement in an edentulous area with deficient dimensions of the alveolar ridge, followed by application of grafting materials and a membrane beneath a soft tissue flap [1–3].

Biomaterials frequently used for GBR like alloplastic bone substitutes, allogenous or autogenous bone are considered as biocompatible, osteoconductive, and have been shown to integrate into newly formed human bone at highly predictable level [4].

Lateral augmentation is a grafting procedure to increase the bone volume of edentulous alveolar ridges showing advanced atrophy, which is conducted prior to or simultaneously with implant insertion. However, histological reports on bone formation after lateral augmentation are scarce and the majority of studies are based on animal trials, as the access to biopsies in these areas is limited [5]. Studies basing on sinus floor

Anton Friedmann and Kirsten Gissel contributed equally to this work.

A. Friedmann · K. Gissel
Department of Periodontology, School of Dentistry, Faculty of Health, Witten-Herdecke University, Witten, Germany

A. Konermann (✉)
Department of Orthodontics, University of Bonn, Bonn, Germany
e-mail: konermann@uni-bonn.de

W. Götz
Department of Orthodontics, Oral Biology Laboratory, University of Bonn, Bonn, Germany

elevations as areas for grafting, which later become donor sites for biopsies, revealed that application of slowly degrading materials exhibits high bone apposition rates of about 20 to 40 % around particulate granules if healing processed uneventfully [6–8]. Though, lateral augmentation procedures regularly experience compromised healing associated with soft tissue dehiscence, premature membrane exposure, and/or exposure of graft and implants [9–11].

Straumann BoneCeramic® is a grafting material that consists of synthetic crystalline biphasic calcium phosphate (BCP) with a mixture of 60 % hydroxylapatite (HA) and 40 % β-tricalciumphosphate (β-TCP), a porosity of ca. 90 % and pores with 100–500 μm in diameter. Morphometrical analyses of BCP performance in a simultaneous grafting approach revealed statistically significant differences in the amount of newly formed mineralized tissues after 6 months in situ when comparing a native non-cross-linked collagen membrane (NCCM) with a ribose cross-linked collagen membrane (RCCM) [12]. In both membrane groups, the healing was compromised in approximately 50 % of the cases although all sites were carefully closed upon augmentation surgery by tensionless adaption of the soft tissue flap.

Histomorphometrical comparison of the integration pattern of BCP in both laterally augmented areas and sinus cavities showed similar values for bone-to-implant contact and for the proportion of newly formed bone [13]. Furthermore, studies evaluating osteoconduction by BCP upon sinus grafting indicate partial resorption of the β-TCP composite component [6–8].

The secondary analysis of the clinical study reported here had two specific objectives: first, to investigate tissue reactions and new bone formation around BCP grafting material both histologically and immunohistochemically and, second, to evaluate whether a history of compromised healing plays a detrimental role in integrating BCP into newly formed tissues and whether premature exposure of the graft contributes to the degradation kinetics of bone substitute materials. Finally, the overall histology of the BCP after 6 months in situ should be evaluated.

Materials and methods

The study was conducted in full accordance with ethical principles, including the World Medical Association Declaration of Helsinki, and with the understanding and written consent of each patient. The study has been independently reviewed and approved by the ethic committee of the Universitätsmedizin Charité, Berlin (Germany) under protocol number EA2/054/05 and registered at ClinicalTrials.gov under ID: NCT00835432.

Patient selection and biopsy retrieval

Specimens included in this study were derived from partially edentulous and generally healthy patients that were non-smokers or smokers with consumption of less than ten cigarettes per day. Each patient exhibited local alveolar ridge atrophy in the intended region of implant surgery and required bone augmentation simultaneous to implant placement. The total sample size investigated in this study comprised 13 sites from 12 patients.

Clinical procedures and biopsy recruitment have been conducted as previously described [12, 13]. In brief, simultaneous augmentation and implant surgery was carried out under local anesthesia (Ultracain DS forte, Aventis, Germany) by a single surgeon (A.F.). Bone dehiscences were treated by using synthetic BCP (Institute Straumann AG, Basel, Switzerland) in combination with a randomly assigned native non-cross-linked collagen membrane (NCCM; BioGide, Geistlich, Wolhusen, Switzerland) or a ribose cross-linked collagen membrane (RCCM; OSSIX, 3i, Palm Beach, FL, USA) for defect seclusion from the flap tissues. Standard Plus Tissue level Straumann implants (SP TL RN; Institute Straumann AG, Basel, Switzerland) were inserted according to the original protocol. Sandblasted, large-grid acid etched (SLA) roughened surfaces were placed at the crestal level of bony ridge making coronal advancement of soft tissue flaps inevitable for covering the area augmented. In consequence, the supracrestal implant portion was submerged and a complete primary closure was achieved. The initial extension of bone defects was assessed clinically by investigator blinded to membrane material inserted and who later was responsible for monitoring the healing period on clinical basis (K.G.).

During 6 months of healing, augmented and implanted regions were clinically monitored for defect healing and tissue conditions. On the basis of these observations, the patient collective was divided into two groups, namely, a collective with uneventfully healed sites and one with compromised healing. Subsequently, the implants were uncovered by repeating flap design and biopsies were harvested from the exposed areas. The harvesting procedure of newly mineralized augmented tissues as much as the amount of tissue obtained was non-standardized, as an equal approach to each surgical site was impossible. The specimens processed for histology in this investigation represent a part of a total patient cohort participating in a former clinical study [12]. For this investigation, only biopsies providing enough material for adequate and valid histological analysis were integrated into the sample collective; for which reason, this study comprises a smaller sample size than the preceding one. The area for biopsy retrieval is presented in Fig. 1.

Fig. 1 Biopsy harvesting. Clinical aspect of re-entry procedure disclosing biopsy retrieval from the augmented zone after 6 months of uneventful healing

Histology and histochemistry

Each sample was fixed by immersion in 4 % buffered formaldehyde (Sörensen buffer) at room temperature (RT) for at least 1 day and subsequently decalcified for about 7 days in 4.1 % disodium ethylene-diamino-tetraacetic acid (EDTA) solution, which was changed every 24 h. After hydration, tissues were dehydrated in an ascending series of ethanol and embedded in paraffin. Serial sagittal sections of 2–3 μm were cut, and representative slides were stained with hematoxylin-eosin (HE), Masson-Goldner trichrome, and PAS staining for histochemical detection of glycosaminoglycans and glycoproteins, respectively. In order to identify osteoclasts, selected tissue sections were stained to demonstrate tartrate-resistant acid phosphatase (TRAP).

Immunohistochemistry

Representative slides from the median parts of the sample series were deparaffinized, rehydrated, and rinsed for 10 min in Tris-buffered saline (TBS). Endogenous peroxidase was blocked in a methanol/H_2O_2 (Merck, Darmstadt, Germany) solution for 45 min in the dark. Sections were pretreated with PBS containing 1 % bovine serum albumin (BSA) for 20 min at RT, digested with 0.4 % pepsin for 10 min at 37 °C and afterwards incubated with the primary antibodies in a humid chamber. Antibody details and incubation protocols are listed in Table 1.

Detection of antibody binding was performed with the peroxidase-conjugated EnVision® anti-mouse system or the EnVision® anti-rabbit/anti-goat HRP-conjugated secondary antibodies (Dako, Glostrup, Denmark) diluted 1:50 and incubated for 30 min at RT. Peroxidase activity was visualized using diaminobenzidine (DAB) yielding a brown staining product and slides were counterstained with Mayer's hematoxylin.

Specificity controls were run by (i) omitting primary antibodies and applying TBS or normal horse serum instead and (ii) omitting primary antibodies or bridge and secondary antibodies, respectively. Mandibular bone or fetal human bone tissues carrying known antigens were used as positive controls.

Immunohistochemical staining intensity was staged semi-quantitatively into (1) no, (2) weak, (3) moderate, (4) strong, and (5) very strong immunostaining.

Two investigators performed the histological evaluations independently and blinded. Each biopsy section stained for conventional or histochemical stainings was analyzed for osteogenesis of the single BCP granules.

Results

Clinical and radiological evaluation

Clinical and radiographic analyses revealed that all implants inserted were osseointegrated and could be loaded with prostheses. Table 2 gives an overview about participants, defect size extensions at phase 1 surgery, membrane assignment, and clinical characteristic of healing. Biopsies included into this analysis are labeled by a footnote cue ([a]). The total sample of 13 sites from 12 patients included seven biopsies from sites with compromised healing and six biopsies from sites with uneventful healing upon augmentation surgery. Figure 2 shows a representative X-ray control of two adjacent implants at re-entry 6 months after installation with GBR. An overview of the biopsy collective investigated with corresponding histological and immunohistochemical findings explicitly described in the following is summarized in Table 3.

Histology and histochemistry

The majority of the specimens investigated disclosed BCP granules with or without surrounding formation of bony structures that were located within a vascularized connective tissue, gingival connective tissue, or alveolar bundle bone. When RCCM membranes were applied, membrane remnants could be identified; however, biopsies only containing membrane remnants were excluded from this study. Due to decalcification processes, the inserted BCP granules appeared empty or only contained some fine granular material. Membraneous osteogenesis around some BCP granules could be observed in nine specimens, of which three biopsies only revealed small perigranular amounts of newly formed osteoid, while the others exhibited more advanced stages of bone formation. In these cases, formation of osteoid or fibrous bone and even

Table 1 List of antibodies. Details of primary antibodies used for immunohistochemistry with corresponding incubation protocols

Antibody	Isotype	Manufacturer	Incubation protocol
Alkaline phosphatase (AP)	Rabbit polyclonal	Quartett (Berlin, Germany)	Ready to use, on, 4 °C
BMP-2	Goat polyclonal	Santa Cruz (Santa Cruz, Ca, USA)	1:25, on, 4 °C
Collagen type I	Mouse monoclonal	Abcam (Cambridge, UK)	1:200, 1 h, rt
ED1 (CD 68)	Mouse monoclonal	Dako (Glostrup, Denmark)	1:100, 1 h, rt
Osteocalcin (OC)	Mouse monoclonal	Takara (Otsu, Shiga, Japan)	1:100, 1 h, rt
Osteopontin (OP)	Rabbit polyclonal	Abcam (Cambridge, UK)	1:200, 1 h, rt
runx2	Goat polyclonal	Santa Cruz (Santa Cruz, Ca, USA)	1:30, on, 4 °C
von Willebrand factor (vWF)	Rabbit polyclonal	Linaris (Wertheim, Germany)	1:200, 1 h, rt

on overnight, *rt* room temperature

remodeling into mature lamellar bone with focal evidence of osteoblasts was evident. On the surfaces of newly formed bone, osteoclasts could focally be observed. In addition, penetration of connective tissue into the BCP material could be registered. Signs of remodeling into lamellar bone were rather observed in specimens from the group with uneventful healing, whereas the group with compromised healing demonstrated low remodeling rates. Osteogenesis was histologically detectable in four out of the seven cases with compromised healing and in five out of the six cases with uneventful healing. The three remaining cases in the first group displayed either missing or minimal osteogenesis, whereas only one sample showed missing osteogenesis in the second group. In these cases with absent osteogenesis around the BCP granules, the material was predominantly covered by dense connective tissue populated by multinuclear cells resembling either osteoclasts or epithelioid giant cells together with intermingled mononuclear cells. The number of giant cells was higher in biopsies from sites with compromised and thus transmucosal healing.

Most of the multinucleated giant cells and macrophages located around BCP granules as much as the osteoclasts detectable along newly formed bone were TRAP positive, although cytoplasmic staining intensity varied between the specimens investigated.

Histological and histochemical results are representatively shown in Fig. 3a–h.

Immunohistochemistry

The staining pattern for ED1 was identical to the TRAP staining, thus labeling all giant cells and macrophages.

Osteoblasts located on newly formed bone were immunoreactive for alkaline phosphatase (ALP). Additionally, weak extracellular staining for ALP could be observed in focal regions of the intergranular connective tissue and along the interfaces between the PCB granules and the perigranular matrix.

Immunostaining for collagen type I appeared in the autochthonous bone as well as in the newly formed bone matrix and the connective tissue matrix.

Newly formed lamellar bone was weakly immunoreactive for osteocalcin (OC), but also, some granular remnants within the granules and the granule interface were stained.

Osteopontin (OP) immunoreactivity was obvious in newly formed bone, but also weakly in the connective tissue. Analogous to OC, granular residual material and interfaces were immunopositive as well.

von Willebrand factor (vWF) immunoreactive vessels were observed in all biopsies investigated. In half of the cases, a very dense vascularization between PCB granules was recorded, however, lacking superiority for any of the groups.

Representative images of each immunohistochemical staining are presented in Fig. 4a–h.

Discussion

In this study, the in vivo performance of a BCP bone substitute material applied in combination with a collagen membrane beneath a soft tissue flap simultaneous to implant insertion in edentulous areas with alveolar ridge atrophy was evaluated by means of histology. In accordance with former studies, the survival rate of the inserted implants was 100 % with evident osseointegration and the potential to be loaded by prosthesis [10, 14]. Simultaneous lateral augmentation tends to achieve new bone formation around previously exposed implant surfaces located within an existing bone defect, of which mineralized defect fill was estimated at an average of 75 % [1, 2, 10]. In turn, this number indicates that almost 25 % of initially exposed implant surfaces are regularly missing osseous formation. Nevertheless, these implants once integrated are lastly considered to be loaded.

As indicated in Table 2, 13 biopsies selected from a total of 38 sites enrolled into the previous study were finally available

Table 2 Overview over the total patient cohort enrolled in the clinical study

Patient number	Age	Sex	Defect size Baseline Depth/width (mm)		Total number of implants	RCCM/NCCM 1/0	Exposure Yes/no 1/0
1	58	F	4	3	3	1	0
2	68	F	5	5	2	1	0
3	64	M	6	5	2	1	1
4	67	F	5	5	2	0	1
5	61	M	7	5	2	1	1
6[a]	47	F	4	8	1	0	1
7	59	F	5	4	1	0	1
8	37	M	7	6	1	1	1
9	62	F	5	4	2	1	1
10	52	F	5	4	2	1	1
11[a]	64	F	8	6	1	0	1
12	44	F	2	4	1	0	0
13[a]	49	F	6	5	2	1	0
14	49	F	5	4	1	0	0
15[a]	40	M	5	6	1	0	0
16	69	M	10	6	1	1	1
17[a]	65	M	7	5	1	1	0
18[a]	65	M	10	15	1	0	1
19[a]	68	F	6	6	2	0	0
20	33	M	10	6	1	1	1
21	63	F	8	5	2	0	1
22	64	F	5	5	2	0	1
23	55	F	4	6	2	1	1
24[a]	40	M	7	6	1	0	1
25	58	F	8	4	1	0	1
26	65	F	7	4	2	0	0
27[a]	56	F	3	5	2	1	1
28[a]	67	F	4	3	2	1	1
29	30	M	10	6	1	0	1
30	67	M	3	3	2	1	0
31	69	F	5	4	2	1	1
32	64	F	3	3	2	1	0
33[a]	69	F	6	4	2	0	0
34	24	M	6	4	1	0	1
35[a]	44	F	8	10	1	1	1
36	49	F	5	7	2	0	0
37	62	F	7	5	2	0	0
38[a]	59	F	1	1	2	0	0

[a] Labels biopsies available for the analysis presented

for this evaluation [12], as most specimens included in the pilot study were classified as inappropriate for the present analysis due to the minimal size of tissues retrieved in some cases. Furthermore, a subgroup of patients included in the pilot study exhibited compromised wound healing, which resulted in premature exposure of bone substitute material to the oral environment. For reason of increased risk for damaging either the implant or the periimplant area, these cases had to be excluded from biopsy harvesting as well. As the pilot study used an undecalcified processing method for specimen preparation, the number of biopsies available from uneventfully healed sites was reduced additionally [13].

In this study, the biopsies were decalcified previously to histological processing, which eliminates the anorganic bone substitute material but has the advantage to stain the sections histochemically and immunhistochemically and to study

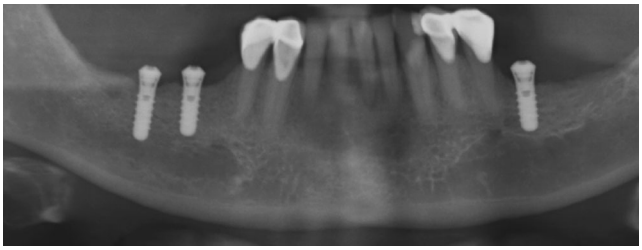

Fig. 2 Radiographic evaluation. Control X-ray documents successful integration of two adjacent implants at re-opening visit

tissues and cellular structures microscopically in a higher resolution [15]. Detection of tissue infiltrates is an additional prerogative for a decalcified approach in histological investigations. In a study evaluating the healing of the same BCP as used in this study after sinus lift, Frenken et al. [16] have also investigated decalcified biopsy specimens, however, using standard histological staining. Immunohistochemical analyses were successfully applied in some animal studies investigating the behavior of ectopic BCP combined with enamel matrix derivative or platelet-derived growth factor in mice [17, 18]. To our knowledge, this study is the first approach presenting immunohistochemical findings from human biopsies retrieved after BCP application, as other studies performed on humans used undecalcified sections for histological evaluation of BCP healing [8, 19, 20].

Our histological results of BCP granule incorporation upon augmentation procedure are similar to findings from other histological investigations on decalcified specimens in humans and animals [16, 18]. In all cases, empty spaces were covered by a dense fibrous, cellular connective tissue with focal appearance of granular material as residues of BoneCeramic®. Additionally, signs related to early osteogenesis could be observed, such as connective tissue invaginations, appearance of ALP-immunoreactive fibroblasts, and osteoblasts in the perigranular area as much as ALP-, OC-, and OP-immunoreactive interfaces between BCP granules and perigranular matrix. These phenomena might involve recruitment of osteogenic cells due to granule surface conditioning for induction of chemoattractive effects [15, 21, 22]. Osteogenic processes around granules observed in this study resembled membraneous osteogenesis with the stages osteoid formation, mineralization, generation of fibrous bone, and later remodeling into mature bone, which demonstrates the osteoconductive property of bone substitute materials as already described in previous studies [13, 16, 23]. Findings from animal experiments could not evidence any osteoinduction upon BCP application, as ectopic bone formation could not be observed [17, 18]. However, our results are in concordance with studies analyzing undecalcified specimens that certify intimate contact between newly formed bone and BCP surfaces, which provides tissue stability and volume preservation as important factors for clinical success of augmentation and implant long-term stability [6, 15, 19]. Other studies analyzed later stages of osteogenesis for the same BCP material and confirmed collagen type I and bone matrix

Table 3 Biopsy collective. Details of the biopsy collective divided into a compromised and an uneventful healing group with corresponding histological and immunohistochemical findings

Patient age (years)	Membrane type	Osteogenesis in augmented areas	Remodeling (TRAP-positive staining)	Giant cells (TRAP-positive staining)	Vessels	Inflammatory infiltrates
Group A (compromised healing)						
67	RCCM	+	(+)	+/+	++	–
49	RCCM	+	(+)/–	(+)/–	+	–
44	RCCM	–	–	–	+	–
64	NCCM	–	–	+/+	(+)	(+)
40	NCCM	–		++/++	+	–
56	NCCM	(+)	(+)/+	(+)/(+)	++	(+)
65	NCCM	+	+	+/+	+/++	(+)
Group B (uneventful healing)						
65	RCCM	(+)	-	+/+		+
47	RCCM	+	(+)/–	(+)/(+)	++	–
68	NCCM	++	(+)/–	(+)/–	+	–
59	NCCM	(+)	(+)/(+)	(+)/–	+	–
69	NCCM	+	(+)/–	(+)/–	+	–
40	NCCM	–	–	(+)/–	+	–

RCCM ribose cross-linked collagen membrane, *NCCM* non-cross-linked collagen membrane

$^{++}$ Very strong occurrence, $^{+}$ strong occurrence, $^{(+)}$ moderate occurrence, $^{-}$ weak occurrence, $^{—}$ no occurrence

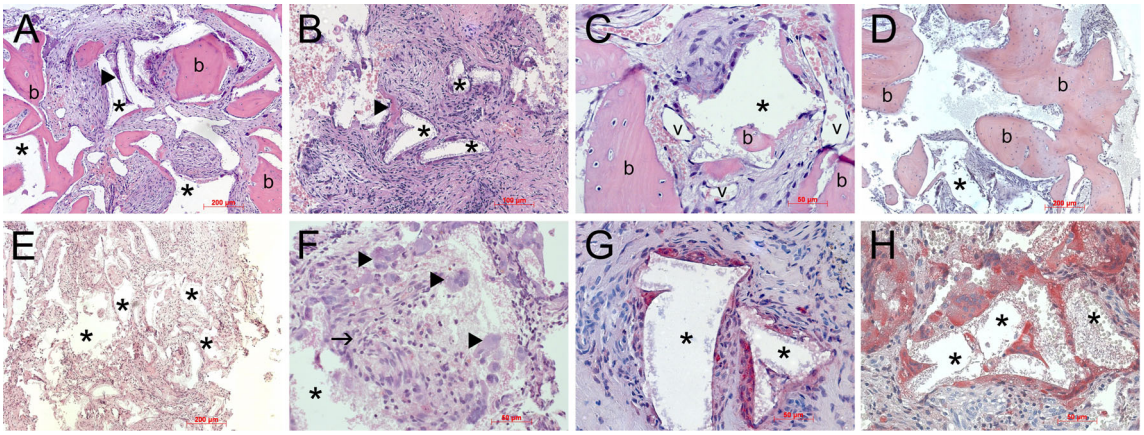

Fig. 3 Histological and histochemical analyses. Magnification is indicated via *bars* on the *lower right* sides of the pictures. **a** Peri- and intergranular bone (*b*) formation within connective tissue that is partly protruding into granules (*arrowhead*). *Asterisks* indicate empty spaces formally occupied by BoneCeramic® granules. H.E. staining. **b** Signs of initial osteogenesis (*arrowhead*) near granules (*asterisks*) within connective tissue. H.E. staining. **c** Granule (*asterisk*) with early perigranular bone formation (*b*) within connective tissue with occurrence of many vessels (*v*). H.E. staining. **d** Advanced bone formation (*b*) next to a granule (*asterisk*). H.E. staining. **e** Area provided by several granules (*asterisks*) without signs of osteogenesis. H.E. staining. **f** Inflammatory infiltrate (*arrow*) and differentiating osteoclasts or giant cells (*arrowheads*) next to a granule (*asterisk*). PAS staining. **g** Accumulation of TRAP-positive multinucleated giant cells (*red*) around granules (*asterisks*). TRAP staining. **h** Distinct accumulation of TRAP-positive multinucleated giant cells (*red*) around granules (*asterisks*). TRAP staining

proteins OC and OP by immunohistochemical detection as components of maturing bone [15, 16]. Presumably, the newly formed bone detected in our investigations already undergoes remodeling processes, which is indicated by the detection of TRAP-positive osteoclasts in close contact to the bony surfaces.

A strong positive reaction for vWF immunostaining as marker for endothelial cells and thus vascularization was evident in both subgroups in this study and confirmed the existence of vascular networks as prerequisite for bone substitute healing and implant osseointegration [24, 25].

The comparison of the descriptive data from both groups of this study revealed rather poorer osteogenesis in the compromised subgroup. Among the specimens from this study, infiltrates were present in three out of seven compromised healed sites, whereas just one out of six submerged healed sites demonstrated infiltration in the biopsy tissue (Tab. 1). Although inflammatory infiltrates were not present in all sites associated with non-submerged healing, premature exposure of the graft may likely be related to inflammation. Accordingly, one of ten sites clinically evaluated for the success of simultaneous GBR along with transmucosal healing of

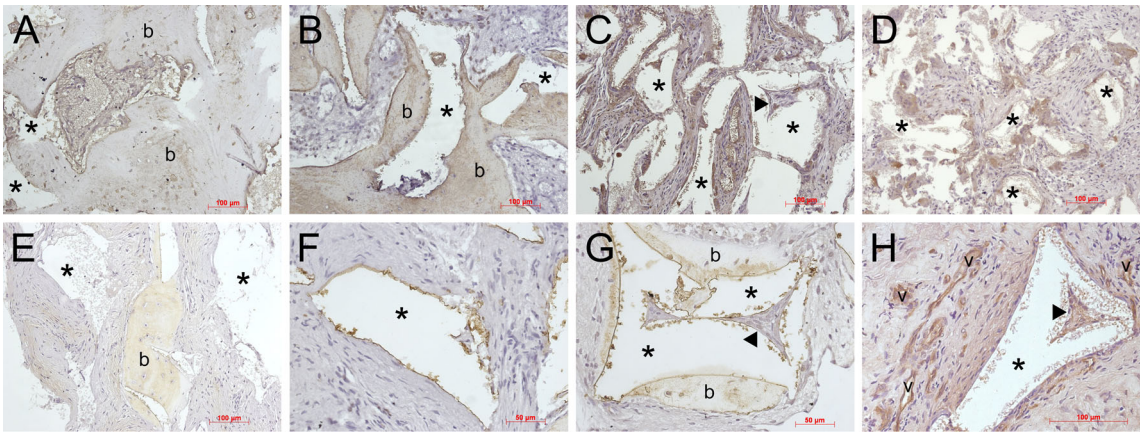

Fig. 4 Immunohistochemical analysis. Magnification is indicated via *bars* on the *lower right* sides of the pictures. Brown staining via DAB. **a** ALP-immunoreactive osteocytes and osteoblasts located on bone (*b*) surfaces. *Asterisks* indicate granules. **b** Collagen type I-immunoreactive perigranular bone (*b*). *Asterisks* indicate granules. **c** ED1-immunoreactive osteoclasts and giant cells located around granules (*asterisks*) that are invaded by tissue protrusions (*arrowhead*). **d** ED1-immunoreactive osteoclasts and giant cells located around granules (*asterisks*). **e** OC-immunoreactive newly formed bone (*b*) near granules (*asterisks*). **f** Interfaces between granule (*asterisk*) and perigranular connective tissue are positively stained for OC. **g** OP-immunoreactive interface and newly formed bone (*b*) around granules (*asterisks*) with occurrence of tissue protrusions (*arrowhead*). **h** vWF-immunoreactive vessels (*v*) around a granule (*asterisk*) occurrence of a tissue protrusion (*arrowhead*)

implants revealed obvious signs of inflammation [26]. The one positive for infiltrate biopsy in the submerged group and one positive from the compromised group belonged to one donor whose general condition turned to be burdened by prostate cancer as evaluated after completion of this study.

Multinucleated giant cells were observed in most cases around granules without surrounding signs of osteogenesis. However, multinuclear giant cell formation due to macrophage fusion is a characteristic for foreign body reactions following early inflammatory cell infiltration [27]; the roles of these cells in bone substitute healing and in degradation of bone ceramics are still unclear [28, 29]. Furthermore, the dissociation from giant cells to osteoclasts is difficult as giant cells cannot clearly be identified by a distinct marker and exhibit variable TRAP activities [29], which could also be observed in this study. Recently, a correlation between the number of multinucleated cells and the vascularization rate has been proposed in an animal model of ectopic bone formation after implantation of TCP granules [30]. There might exist a correlation between premature material exposure and the development of these cells, since a tendency to higher numbers in cases with compromised healing was noticed in our study. Future research will be necessary to clarify their role in the degradation processes of bone substitute materials.

Our results confirm the suitability of BCP material to effectively support bone formation in simultaneous augmentation procedures. However, premature exposure of the bone substitutes diminishes the outcome in terms of new bone gain and bears a risk of an inflammatory tissue reaction.

Acknowledgments We thank Mrs. Inka Müller-Bay for technical assistance.

Conflict of interest The authors declare that they have no conflict of interest.

References

1. Jensen SS, Terheyden H (2009) Bone augmentation procedures in localized defects in the alveolar ridge: clinical results with different bone grafts and bone-substitute materials. Int J Oral Maxillofac Implants 24(Suppl):218–236
2. Donos N, Mardas N, Chadha V (2008) Clinical outcomes of implants following lateral bone augmentation: systematic assessment of available options (barrier membranes, bone grafts, split osteotomy). J Clin Periodontol 35:173–202
3. Retzepi M, Donos N (2010) Guided bone regeneration: biological principle and therapeutic applications. Clin Oral Implants Res 21: 567–576
4. Kolk A, Handschel J, Drescher W, Rothamel D, Kloss F, Blessmann M, Heiland M, Wolff KD, Smeets R (2012) Current trends and future perspectives of bone substitute materials—from space holders to innovative biomaterials. J Craniomaxillofac Surg 40:706–718
5. Tal H, Artzi Z, Kolerman R, Beitlitum I, Goshen G (2012) Augmentation and preservation of the alveolar process and alveolar ridge of bone. Bone Regeneration, InTech Rijeka, pp 139–184
6. Cordaro L, Bosshardt DD, Palattella P, Rao W, Serino G, Chiapasco M (2008) Maxillary sinus grafting with Bio-Oss or Straumann Bone Ceramic: histomorphometric results from a randomized controlled multicenter clinical trial. Clin Oral Implants Res 19:796–803
7. Artzi Z, Kozlovsky A, Nemcovsky CE, Weinreb M (2005) The amount of newly formed bone in sinus grafting procedures depends on tissue depth as well as the type and residual amount of the grafted material. J Clin Periodontol 32:193–199
8. Schmitt CM, Doering H, Schmidt T, Lutz R, Neukam FW, Schlegel KA (2013) Histological results after maxillary sinus augmentation with Straumann®, BoneCeramic, Bio-Oss®, Puros®, and autologous bone. A randomized controlled clinical trial. Clin Oral Implants Res 24:576–585
9. Becker J, Al-Nawas B, Klein MO, Schliephake H, Terheyden H, Schwarz F (2009) Use of a new cross-linked collagen membrane for the treatment of dehiscence-type defects at titanium implants: a prospective, randomized-controlled double-blinded clinical multicenter study. Clin Oral Implants Res 20:742–749
10. Moses O, Pitaru S, Artzi Z, Nemcovsky CE (2005) Healing of dehiscence-type defects in implants placed together with different barrier membranes: a comparative clinical study. Clin Oral Implants Res 16:210–219
11. Schwarz F, Hegewald A, Sahm N, Becker J (2013) Long-term follow-up of simultaneous guided bone regeneration using native and cross-linked collagen membranes over 6 years. Clin Oral Implants Res. doi:10.1111/clr.12220
12. Friedmann A, Gissel K, Soudan M, Kleber BM, Pitaru S, Dietrich T (2011) Randomized controlled trial on lateral augmentation using two collagen membranes: morphometric results on mineralized tissue compound. J Clin Periodontol 38:677–685
13. Friedmann A, Dard M, Kleber BM, Bernimoulin JP, Bosshardt DD (2009) Ridge augmentation and maxillary sinus grafting with a biphasic calcium phosphate: histologic and histomorphometric observations. Clin Oral Implants Res 20:708–714
14. Jung RE, Windisch SI, Eggenschwiler AM, Thoma DS, Weber FE, Hammerle CH (2009) A randomized-controlled clinical trial evaluating clinical and radiological outcomes after 3 and 5 years of dental implants placed in bone regenerated by means of GBR techniques with or without the addition of BMP-2. Clin Oral Implants Res 20: 660–666
15. Götz W, Gerber T, Michel B, Lossdörfer S, Henkel KO, Heinemann F (2008) Immunohistochemical characterization of nanocrystalline hydroxyapatite silica gel (NanoBone(r)) osteogenesis: a study on biopsies from human jaws. Clin Oral Implants Res 19:1016–1026
16. Frenken JW, Bouwman WF, Bravenboer N, Zijderveld SA, Schulten EA, ten Bruggenkate CM (2010) The use of Straumann Bone Ceramic in a maxillary sinus floor elevation procedure: a clinical, radiological, histological and histomorphometric evaluation with a 6-month healing period. Clin Oral Implants Res 21:201–208
17. Chan RC, Marino V, Bartold PM (2012) The effect of Emdogain and platelet-derived growth factor on the osteoinductive potential of hydroxyapatite tricalcium phosphate. Clin Oral Investig 16:1217–1227
18. Mrozik KM, Gronthos S, Menicanin D, Marino V, Bartold PM (2012) Effect of coating Straumann Bone Ceramic with Emdogain on mesenchymal stromal cell hard tissue formation. Clin Oral Investig 16:867–878
19. Mardas N, Chadha V, Donos N (2010) Alveolar ridge preservation with guided bone regeneration and a synthetic bone substitute or a bovine-derived xenograft: a randomized, controlled clinical trial. Clin Oral Implants Res 21:688–698
20. Iezzi G, Degidi M, Piattelli A, Mangano C, Scarano A, Shibli JA, Perrotti V (2012) Comparative histological results of different

biomaterials used in sinus augmentation procedures: a human study at 6 months. Clin Oral Implants Res 23:1369–1376
21. Boyan BD, Bonewald LF, Paschalis EP, Lohmann CH, Rosser J, Cochran DL, Dean DD, Schwartz Z, Boskey AL (2002) Osteoblast-mediated mineral deposition in culture is dependent on surface microtopography. Calcif Tissue Int 71:519–529
22. Knabe C, Koch C, Rack A, Stiller M (2008) Effect of beta-tricalcium phosphate particles with varying porosity on osteogenesis after sinus floor augmentation in humans. Biomaterials 29:2249–2258
23. de Lange GL, Overman JR, Farré-Guasch E, Korstjens CM, Hartman B, Langenbach GE, Van Duin MA, Klein-Nulend J (2014) A histomorphometric and micro-computed tomography study of bone regeneration in the maxillary sinus comparing biphasic calcium phosphate and deproteinized cancellous bovine bone in a human split-mouth model. Oral Surg Oral Med Oral Pathol Oral Radiol 117:8–22
24. Koerdt S, Siebers J, Bloch W, Ristow O, Kuebler AC, Reuther T (2013) Immunohistochemial study on the expression of von Willebrand factor (vWF) after onlay autogenous iliac grafts for lateral alveolar ridge augmentation. Head Face Med 9:40
25. Götz W, Reichert C, Canullo L, Jäger A, Heinemann F (2012) Coupling of osteogenesis and angiogenesis in bone substitute healing—a brief overview. Ann Anat 194:171–173
26. Hammerle CH, Lang NP (2001) Single stage surgery combining transmucosal implant placement with guided bone regeneration and bioresorbable materials. Clin Oral Implants Res 12:9–18
27. Anderson JM, Rodriguez A, Chang DT (2008) Foreign body reaction to biomaterials. Semin Immunol 20:86–100
28. Chappard D, Guillaume B, Mallet R, Pascaretti-Grizon F, Baslé MF, Libouban H (2010) Sinus lift augmentation and ß-TCP: a microCT and histological analysis on human bone biopsies. Micron 41:321–326
29. Kucera T, Sponer P, Urban K, Kohout A (2013) Histological assessment of tissue from large human bone defects repaired with ß-tricalcium phosphate. Eur J Orthop Surg Traumatol In press.
30. Ghanaati S, Barbeck M, Ort C, Willershausen I, Thimm BW, Hoffmann C, Rasic A, Sader RA, Unger RE, Peters F, Kirckpatrick CJ (2010) Influence of ß-tricalcium phosphate granule size and morphology on tissue reaction in vivo. Acta Biomater 6:4476–4487